

Regular and chaotic motions of Chaplygin sleigh with periodically switched nonholonomic constraint

Sergey P. Kuznetsov

*Udmurt State University, Universitetskay 1,
Izhevsk, 426034, Russian Federation*

*Saratov Branch of Kotelnikov's Institute of Radio-Engineering and Electronics of RAS,
Zelenaya 38, Saratov, 410019, Russian Federation*

PACS 05.45.-a

Nonlinear dynamics and chaos

PACS 45.40.-f

Dynamics and kinematics of rigid bodies

Abstract – We consider motions of Chaplygin sleigh on a plane supposing that the nonholonomic constraint is located periodically turn by turn at each of three legs supporting the sleigh. We assume that at switching on the constraint the respective element (“knife edge”) is directed along the local velocity vector and becomes fixed relative to the sleigh for a certain time interval till the next switch. Differential equations of the mathematical model are formulated and analytical derivation of 2D map for the state transformation on the switching period is provided. The dynamics takes place with conservation of the mechanical energy. Numerical simulations show phenomena characteristic to nonholonomic systems with complex dynamics (rattleback etc.). In particular, on the energy surface attractors occur responsible for regular sustained motions settling in domains of prevalent area compression by the map. In addition, chaotic and quasiperiodic regimes take place similar to those observed in conservative nonlinear dynamics.

Study of complex dynamics of nonlinear systems, including dynamic chaos, is one of the fundamental interdisciplinary problems. To date, extensive material has been accumulated, including many theoretical results, methodologies and analysis algorithms, a variety of examples of model systems with complex dynamics, experimental data, etc. [1-3].

A productive approach within this scientific direction consists in development of generalized models covering some range of phenomena and applicable, at least for qualitative description of systems of different nature. As a sample, we refer to the standard Chirikov-Taylor 2D-map relating to conservative Hamiltonian systems [4-6]. A simple concrete example is a mechanical rotator, a rod fixed with the hinge at the end undergoing a plane rotational motion induced by periodic short kicks of the external force. With small nonlinearity, regular quasiperiodic motions dominate represented by invariant curves on the phase plane (they are associated with KAM tori), and chaos occurs in narrow stochastic layers separated by areas of regular dynamics. With increase of the nonlinearity parameter, the regions of chaotic motion enlarge, forming a "chaotic sea" surrounding the surviving islands of regular dynamics. Note that the Liouville theorem is fulfilled: the phase volume element in the two-dimensional space is preserved under iterations of the map. An analogous model usually called the Zaslavsky map is also introduced for systems with dissipation [4, 3]. Dynamics in this case is accompanied by contraction of the phase volume. Steady motions correspond to attractors e.g. the attracting invariant curves and fixed points at weak nonlinearity, and the chaotic attractors typical for strong nonlinearity.

In mechanics, besides the systems described in the framework of the Hamiltonian formalism (conservative) and systems with friction (dissipative), another special class of systems with nonholonomic constraints is considered [7,8]. They include many situations of great practical value, for example, in the analysis of mobile vehicles, e.g. in the context of robotics. Hierarchy of types of behavior of nonholonomic systems include a variety ranging from simple (integrable) to complex (nonintegrable) cases, which is associated with a number of inherent invariants and symmetries [9,10]. A typical example is motion of a solid body with a convex smooth surface on a rough plane (the rattleback, or the Celtic stone [11]). A fundamental property of Celtic stone and other non-holonomic systems occupying a similar place in the

hierarchy is that they do not possess invariant measure in the sense of the Liouville theorem [12]. Although the system is conservative (conservation of mechanical energy) and symmetric with respect to time reversal, the phase volume elements during the dynamic evolution do not remain constant, locally undergoing compression or expansion in some places of the phase space. Due to this, the asymptotic behaviors associated with attractors can occur, like those in dissipative systems [13-15]. From a general point of view, this special class occupies an intermediate position between the conservative and dissipative systems and deserves attention in the framework of the theory of dynamical systems [16]. In particular, it would be desirable and interesting to introduce models similar to those of Chirikov – Taylor and Zaslvsky, but expressing the specific character of the nonholonomic dynamics.

One of paradigmatic examples of the non-holonomic mechanics is Chaplygin sleigh [17-21]. It is a solid body that can move on a plane surface, having a “knife edge” attached to the sleigh as one of the supports, capable of sliding only in the longitudinal direction. The dynamics of the classical model with some initial translational and angular velocity leads to arising steady motion of the sleigh at a constant speed in the direction of the knife edge. For the sleigh moving in presence of weak dissipation under supplied periodic pulses of torque, a possibility of complex dynamics was noted in [21].

In this paper, we propose a modification of the Chaplygin sleigh problem, which makes possible complex dynamics with conservation of mechanical energy and leads to a model 2D map that can pretend to be a non-holonomic analog of the standard mapping.

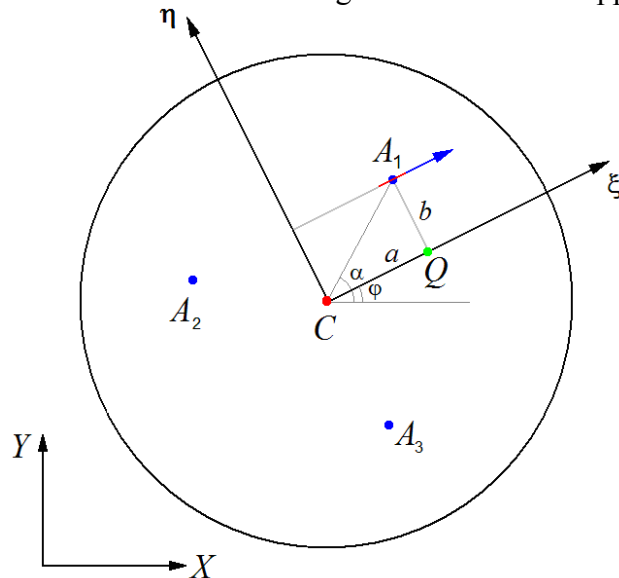


Figure 1: Chaplygin sleigh moving on the plane. The laboratory frame (X, Y) , and the sleigh-referenced frame (ξ, η) with the origin at the center of mass C are used. A situation shown corresponds to location of the non-holonomic constraint at A_1 (the knife-edge shown as the red segment). The point Q is a specially defined point of the sleigh, which velocity in the knife-edge direction is one of the variables in the dynamic equations. A_2 and A_3 are the points where the non-holonomic constraints impose on other stages of the motion.

Consider the Chaplygin sleigh moving the horizontal plane, assuming that the conditions of the non-holonomic mechanical constraints are imposed turn by turn for time intervals of duration T at the points of the sleigh A_1, A_2, A_3 located at the vertices of an equilateral triangle and at distance r from the center of mass (Fig.1). While the constraint is supplied, the speed of the corresponding vertex is oriented in a direction fixed relative to the sleigh defined as the direction of the local velocity of this point at the switching on the constraint. One can imagine this in such way that the supports providing contact of the sleigh with the plane are fabricated as knife-edges installed at A_1, A_2, A_3 on the hinges attached to the sleigh, one of which is fixed for a time T while others can rotate freely. While there is no fixation, the presence of the knife-edge does not affect the motion of the sleigh, but it keeps orientation along the local velocity vector. With the

fixation, the rotation of the knife-edge stops, and the non-holonomic constraint appears to be imposed.

Description of the motion consists of three periodically repeating stages corresponding to the constraints imposed at the points A_1, A_2, A_3 . At each of these stages one can use the Chaplygin sleigh equations in the form provided by Borisov and Mamaev [19]. For this, it is needed to determine variables and parameters appearing in these equations, and redefine them at each new stage.

Suppose that in beginning of the stage the state of the system is given by a set of variables

$$(X_C, Y_C, U_C, V_C, \omega, \alpha), \quad (1)$$

where (X_C, Y_C) are coordinates of the center of mass in the laboratory frame, (U_C, V_C) are the components of the velocity of the center of mass in projection on the X and Y axes, ω is instantaneous angular velocity of the sleigh, and α is angle of the radius vector of the point of application of the constraint A with the X axis. Then the coordinates of A are

$$X_A = X_C + r \cos \alpha, \quad Y_A = Y_C + r \sin \alpha, \quad (2)$$

where r is the distance from the center of mass, and the velocity components are

$$U_A = U_C - \omega r \sin \alpha, \quad V_A = V_C + \omega r \cos \alpha. \quad (3)$$

at the initial moment, the direction of the knife-edge is fixed relative to the sleigh, having an angle to the X axis

$$\varphi = \arg(U_A + iV_A), \quad (4)$$

while the absolute value of the velocity is given by

$$u_A = \sqrt{U_A^2 + V_A^2}. \quad (5)$$

Then, we define an orthogonal coordinate system with origin at the center of mass C so that the ξ -axis is parallel to the knife-edge. The coordinates of the point A are, obviously,

$$\xi_A = a = r \cos \theta, \quad \eta_A = b = r \sin \theta, \quad (6)$$

where $\theta = \alpha - \varphi$. The projection of the velocity on the ξ axis is given by the above expression for u_A , and the projection onto the η axis is zero: $v_A=0$. Parameters (a, b, θ) remain constant throughout the considered stage, but in other stages they generally will be different.

To simplify the equations, it is convenient to select a special point Q as projection of the point of application of the constraint onto the axis of the sleigh-referenced coordinate system ξ [19]. The coordinates and velocity components in the laboratory system are

$$X_Q = X_C + a \cos \varphi, \quad Y_Q = Y_C + a \sin \varphi, \quad (7)$$

$$\begin{aligned} U_Q &= U_C - a\omega \sin \varphi = U_A + \omega r \sin \alpha - a\omega \sin \varphi, \\ V_Q &= V_C + a\omega \cos \varphi = V_A - \omega r \cos \alpha + a\omega \cos \varphi. \end{aligned} \quad (8)$$

Respectively, for the velocity projections on the coordinate axes of the sleigh-referenced frame ξ and η we have

$$\begin{aligned} u &= U_Q \cos \varphi + V_Q \sin \varphi = u_A + \omega r \sin \alpha \cos \varphi - \omega r \cos \alpha \sin \varphi = u_A + \omega r \sin(\alpha - \varphi) = u_A + b\omega, \\ v &= -U_Q \sin \varphi + V_Q \cos \varphi = v_A - \omega r \sin \alpha \sin \varphi + \omega r \cos \alpha \cos \varphi + a\omega = v_A = 0. \end{aligned} \quad (9)$$

The resulting set of values $(u, \omega, \varphi, X_Q, Y_Q)$ sets the initial conditions for the equations [19]

$$\begin{aligned}
\dot{u} &= a\omega^2, \\
(\mu + a^2)\dot{\omega} &= -a\omega u, \\
\dot{\varphi} &= \omega, \\
\dot{X}_Q &= u \cos \varphi, \dot{Y}_Q = u \sin \varphi,
\end{aligned} \tag{10}$$

where $\mu = J/m$ is a ratio of the moment of inertia of the sleigh to the mass.

Equations (12) must be integrated over a time interval T , and then the resulting set of variables $u, \omega, \varphi, X_Q, Y_Q$ makes it possible to define the final state in the same form as the initial state. Notice that a shift $2\pi/3$ must be added to the angular variable, which corresponds to switching fixation of the non-holonomic constraint to another place. As a result, we have

$$\begin{aligned}
&(X_C, Y_C, U_C, V_C, \omega, \alpha)_{new} = \\
&= (X_Q - a \cos \varphi, Y_Q - a \sin \varphi, u \cos \varphi + a\omega \sin \varphi, u \sin \varphi - a\omega \cos \varphi, \omega, \varphi + \theta + 2\pi/3). \tag{11}
\end{aligned}$$

На всех стадиях эволюции выполняется сохранение механической энергии
At all stages of evolution, the mechanical energy

$$W = \frac{1}{2}m(U_C^2 + V_C^2) + \frac{1}{2}J\omega^2 \equiv \frac{1}{2}m[u^2 + (\mu + a^2)\omega^2] \tag{12}$$

is conserved. From the parameters of the problem m, r, J, T and the energy W one can compose two dimensionless combinations

$$P_1 = \frac{J}{mr^2}, \quad P_2 = \sqrt{\frac{2W}{m}} \frac{T}{r}, \tag{13}$$

which are similarity criteria for the sleigh dynamics in our formulation of the problem. Subsequently, the mass of the sleigh m and the distance r are always taken equal to unity, which does not violate generality of the analysis; then, $P_1 = \mu, P_2 = \sqrt{2WT}$.

First, let's concentrate not in motions in real space, but in classification of types of the dynamic behavior (periodic and quasi-periodic movements, chaos). To reduce the description one can use the fact that the first three equations (12) form a separate set independent of the last two equations, and allow analytical integration. Since the energy W given by the relation (13) conserves, we seek the solution in a form

$$u = \sqrt{2W} \cos \Phi, \quad \omega = \sqrt{2W}(\mu + a^2)^{-1/2} \sin \Phi. \tag{14}$$

Then for the variable Φ we obtain an equation with separable variables

$$\dot{\Phi} = -a\sqrt{2W}(\mu + a^2)^{-1} \sin \Phi, \tag{15}$$

and integration yields

$$\tan \frac{\Phi(t)}{2} = \tan \frac{\Phi_0}{2} \exp\left(-\frac{\sqrt{2W}a}{\mu + a^2} t\right), \tag{16}$$

where $\Phi_0 = \arg[u + i\omega(\mu + a^2)^{1/2}]_{t=0}$. Next, we note that

$$\dot{\varphi} = \omega = \sqrt{2W}(\mu + a^2)^{-1/2} \sin \Phi = -a^{-1}(\mu + a^2)^{1/2} \dot{\Phi}, \tag{17}$$

and, hence, $\varphi(t) - \varphi_0 = -a^{-1}(\mu + a^2)^{1/2}(\Phi(t) - \Phi_0)$. Finally, we have

$$\begin{aligned}
u(T) &= \sqrt{2W} \cos \Phi(T), \\
\omega(T) &= \sqrt{2W} (\mu + a^2)^{-1/2} \sin \Phi(T), \\
\varphi(T) &= \varphi_0 + a^{-1} (\mu + a^2)^{1/2} (\Phi(T) - \Phi_0),
\end{aligned} \tag{18}$$

and substituting these values in (14) we obtain the required result, the state at the instant of the next switching.

Taking into account invariance with respect to rotations in the plane and conservation of energy W , which naturally appears as a parameter, the problem can be reduced to 2D mapping.

For dynamic variables at the switching we take the angular velocity normalized to its maximal possible value $w_n = \omega(nT) \sqrt{\mu/2W}$, and the angle between the direction of the velocity of the center of mass and the radius vector of the point where the constraint is currently imposed $\gamma_n = \arg[U_c(nT) + iV_c(nT)] - \alpha(nT)$. Using results of the analytical solution, one can write down the map describing the state change over a period T in a following compact form:

$$\gamma_{n+1} = \arg \left[U \left(1 - G^2 - \frac{2iaG}{\sqrt{\mu + a^2}} \right) \right] - \frac{2\pi}{3}, \quad w_{n+1} = \frac{2G}{(1 + G^2) \sqrt{1 + \mu^{-1} a^2}}, \tag{19}$$

where

$$U = \sqrt{1 - w_n^2} \exp(i\gamma_n) + i\mu^{-1/2} w_n, \quad a = |U|^{-1} \operatorname{Re} U, \quad G = \frac{w_n \sqrt{\mu + a^2} \exp\left(-\frac{aT\sqrt{2W}}{\mu + a^2}\right)}{\mu^{1/2} + \mu^{1/2} |U| - w_n |U|^{-1} \operatorname{Im} U}$$

To illustrate characteristic dynamic modes depending on initial conditions, we choose the parameters $T=5$, $\mu=3$, $2W=1.5129$, which correspond to $P_1=3$, $P_2=6.15$.

Figure 2 shows diagram in the plane of variables (γ, ω) obtained by iterations of the map (19) using a representative set of initial conditions. Like the Chirikov-Taylor map, it demonstrates invariant curves either going from the left to the right border, or appearing as closed formations. Also, a "chaotic sea" takes place in the bottom part of the diagram. The principal difference, however, is presence of objects of a different type, which are more characteristic for dissipative dynamics.

First of all, in the top part of the diagram there is a fixed point A ($\gamma=3.07152006$, $\omega=0.51302349$), which is an attractor. Basin of attraction, i.e. the set of starting points of the orbits going to the attractor is shown around the attractor by uniform tone (pink in this color figure on-line). Along with the attractor, there is a repeller – a fixed point R ($\gamma=4.25886280$, $\omega=0.51302349$), to which the orbits arrive with iterations in the inverse time for a certain set of initial conditions.

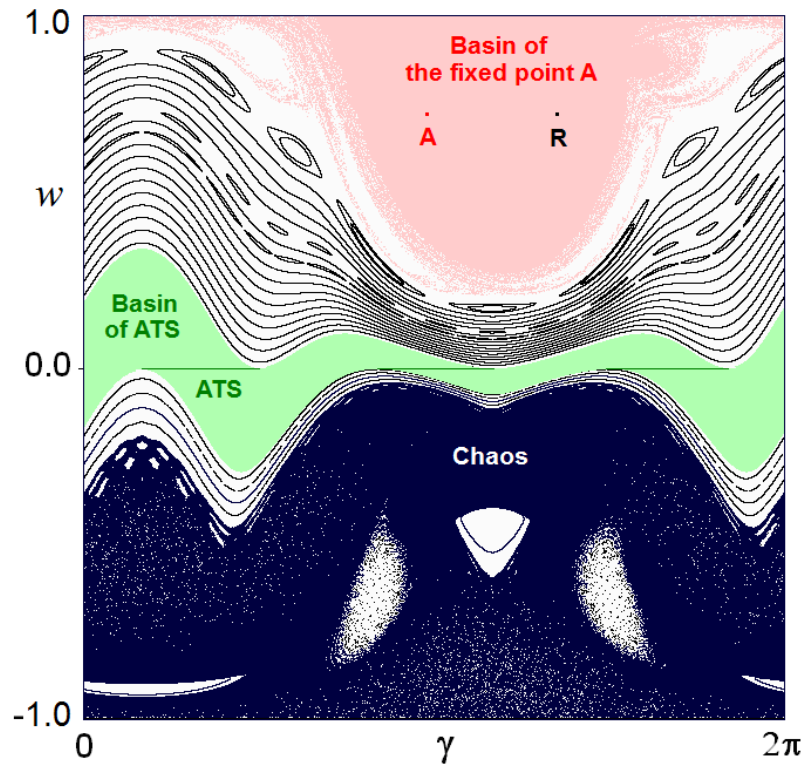


Figure 2 (color on-line): Phase portrait of the map (19) on the plane (γ, ω) at $T=5$, $\mu=3$, $2W=1.5129$. Black curves represent quasiperiodic motions corresponding to quasi-conservative dynamics; the same curves are obtained when solving the problem in the inverse time. A vast dark area in the lower part of the diagram is "chaotic sea". A light green area is a basin of attraction of the family of trivial motions ATS placed on the axis $w=0$. Pink region is the attraction basin of the fixed point A. The fixed point R is repulsive.

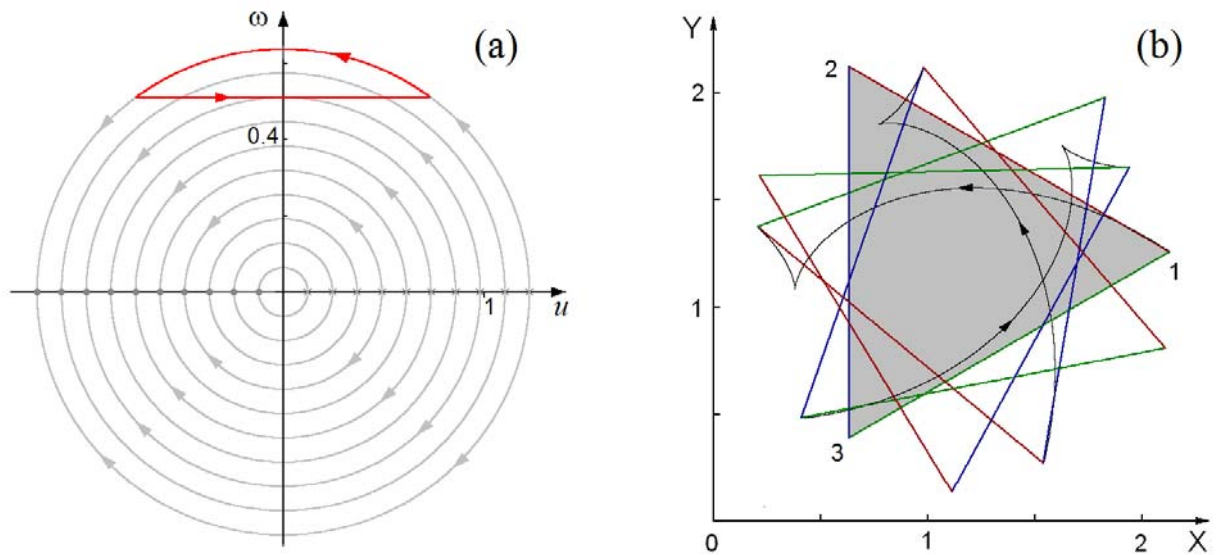


Fig.3. Portrait in projection on the phase plane of the differential equations describing motion in time intervals between switches, where the bold red contour shows the corresponding attractor, the limit cycle (a) and the diagram illustrating real motion of the sleigh on the plane associated with the attractor (b) at $T=5$, $\mu=3$, $2W=1.5129$.

The fixed point corresponds to the fact that in the stage of continuous motion described by differential equations, the values (u_0, w_0) of the variables change to $(-u_0, w_0)$ (Fig. 3a). At the end of the stage, the angle between the velocity vector and the radius vector of the point of application of the constraint relative to the center of mass coincides with the initial value. The fixed point of the map corresponds to a cyclic evolution in the continuous time for the angular

velocity and the projection of the velocity in the sleigh reference frame. As can be shown, the attractor, the fixed point (along with the repeller), takes place in a certain range of energies as defined by

$$2\sqrt{3\mu} < \sqrt{2WT} < 2(\mu+1) \ln \left(\sqrt{1 + \frac{3}{\mu+1}} + \frac{\sqrt{3}}{\sqrt{\mu+1}} \right). \quad (20)$$

The upper limit of W corresponds to the bifurcation of merge and disappearance of the pair of the fixed points. The lower bound is associated with such a situation that the velocity vector of the point when the constraint is supplied is orthogonal to the radius vector, and the parameter a vanishes. Actually, motion of the sleigh in real space corresponding to the attractor of the 2D map is quasi-periodic because of the fact that the angle of rotation over the switching period, generally, is not in rational relative to the value of 2π (fig.3b).

Further, there is a trivial attracting set of points ATS on the horizontal axis $w=0$, indicated in Fig. 2 by horizontal segments of green color. (The orbits visit these segments in turn during iterations of the map.) Such motions, when there are no rotations, and the translational velocity is constant, can continue for infinitely long time accompanied only by changes of location of the active knife-edges without modifying their orientation in the laboratory reference system. This corresponds to the family of fixed points of the 2D map $(w, \gamma) = (0, \text{const})$ for the total switching period $3T$.

Basin of attraction for the family of trivial motions in the plane (γ, w) is a wave-shaped strip containing the axis $w=0$ is indicated in Fig.3 by light green color. Note that in respect to horizontal shifts along the axis $w=0$ the neutral stability occurs; actually we deal not with a single attractive fixed point, but with a set of fixed points filling certain segments. The rest of the axis $w=0$ is occupied by repelling fixed points.

The mapping (23), although obtained for a system with energy conservation, does not belong to the area-preserving class that can be verified directly by numerical computation of the Jacobi determinant $D = \partial(\gamma_{n+1}, w_{n+1}) / \partial(\gamma_n, w_n)$ in the region $-1 < w_n < 1$, $0 \leq \gamma_n < 2\pi$. The attractive point falls into the region where the map is compressive. The repeller point sits in the region where the map is expansive. Quasi-conservative motions represented by the invariant curves and the chaotic sea correspond to orbits visiting equally often the areas of compression and expansion. The trivial attracting set of points on the axis consists of three segments visited in turn, two of which fall into the region of compression, which guarantees the attractive nature of this set.

With conventional methods described in the literature [1, 3, 22] one can compute Lyapunov exponents for different orbits., For the fixed point A two Lyapunov exponents are negative ($\Lambda_1 = -0.1584$, $\Lambda_2 = -2.3098$ for parameters corresponding to Fig.2), while for the repeller R they are positive ($\Lambda_1 = 2.3098$, $\Lambda_2 = 0.1584$). For the invariant curves both two Lyapunov exponents are zero up to computing errors. For the "chaotic sea" one exponent is positive, indicating chaotic nature of the dynamics, and the second is given by a negative number equal in the absolute value: $\Lambda_1 = 0.489$, $\Lambda_2 = -0.489$. (The Lyapunov exponents are given determined for the full period of switching $3T$.) For motions without rotation, i.e., at the axis $w=0$ one Lyapunov exponent is always zero (it corresponds to a shift in the angular variable γ), a nontrivial second exponent is given by

$$\Lambda = -\sqrt{2WT} \left(\frac{\cos \gamma}{\mu + \cos^2 \gamma} + \frac{\cos(\gamma + 2\pi/3)}{\mu + \cos^2(\gamma + 2\pi/3)} + \frac{\cos(\gamma + 4\pi/3)}{\mu + \cos^2(\gamma + 4\pi/3)} \right). \quad (21)$$

It is negative in the following intervals: $\gamma \in (\pi/6, \pi/2)$, $(5\pi/6, 7\pi/6)$, $(3\pi/2, 11\pi/6)$.

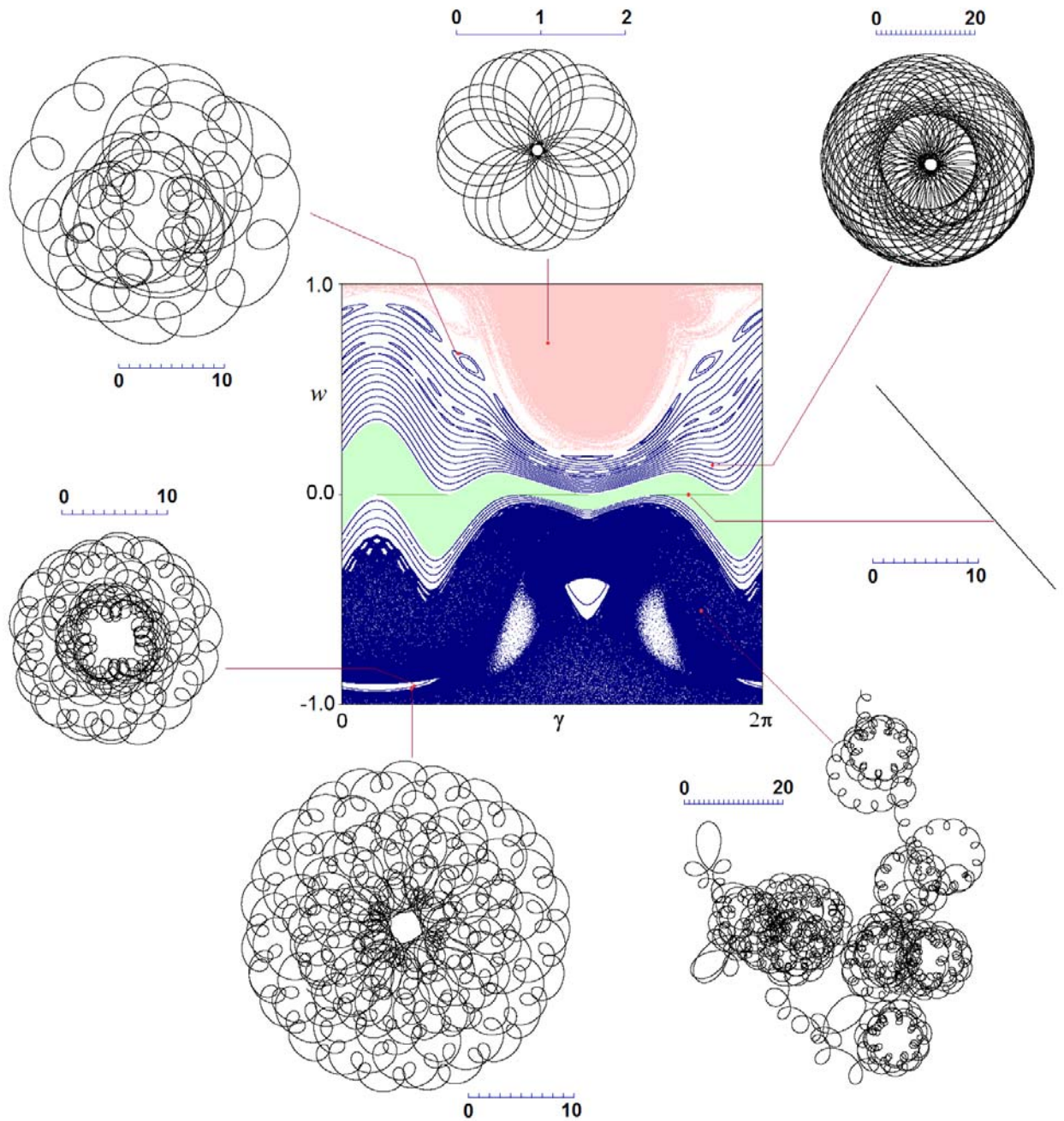


Figure 4: Pictures on the periphery depict trajectories of the center of mass of the sleigh corresponding to representative points of the phase plane of the 2D map shown in the center. The parameters are $T=5$, $\mu=3$, $2W=1.5129$.

In Fig. 4, the middle diagram reproduces the phase plane of the 2D map at $T=5$, $\mu=3$, $2W=1.5129$, and on the periphery of the figure pictures are presented showing trajectories of the center of mass in the laboratory reference frame corresponding to representative types of motion. (The initial data in the phase plane for the angular velocity w and the angular variable γ are indicated by pointers.) Shown in the right below figure is chaotic, diffusion-like motion of the sleigh containing numerous curls corresponding to the chaotic sea.

Summing up, the work considers motions of Chaplygin's sleigh with periodic swathing the place of application of the non-holonomic constraint, located successively in one of the three supports in the vertices of an equilateral triangle. A two-dimensional map is obtained that takes the place of the standard Chirikov – Taylor map for the non-holonomic system. The possibility of regular and chaotic motions is shown depending on parameters and initial conditions. In particular, stable motions are possible associated with attractors in the phase space of the reduced system of equations for translational and angular velocities. Regular and chaotic modes similar

to conservative dynamics also occur represented by families of invariant curves and "chaotic sea".

It may be supposed that the present material opens some prospects for design of mobile devices with nontrivial dynamical properties, e.g. in the context of robotics. Particularly, due to occurrence of chaotic modes it may be expected that effective managing the sleigh motions using the chaos control techniques [22-24] will be possible.

This work was supported by a grant of Russian Science Foundation No 15-12-20035. The author is grateful to A.V. Borisov, who offered to look for an analog of standard Chirikov – Taylor map appropriate to nonholonomic mechanics, in particular, to the dynamics of the Chaplygin sleigh, and to A.A. Kilin and I.S. Mamaev for useful discussion.

References

- [1] Schuster H.G. and Just W. *Deterministic Chaos: An Introduction*. Wiley-VCH, 2005. 312 p.
- [2] Guckenheimer J., Holmes P. J. *Nonlinear oscillations, dynamical systems, and bifurcations of vector fields*. – Springer Science & Business Media, 2013.
- [3] .P.Kuznetsov. *Dynamical Chaos*. Moscow: Fizmatlit. 2001. (In Russian.)
- [4] R.Z. Sagdeev, D.A. Usikov, and G.M. Zaslavskii. *Nonlinear physics: from the pendulum to turbulence and chaos*. Harwood Academic, 1990.
- [5] A.J.Lichtenberg, M.A.Lieberman, "Regular and chaotic dynamics", Springer, Berlin (1992).
- [6] L.E.Reichl, "The Transition to chaos in conservative classical systems and quantum manifestations", Springer, Berlin (2004).
- [7] Neimark Ju. I. and Fufaev N. A. *Dynamics of Nonholonomic Systems*, Translations of Mathematical Monographs, Vol. 33 (American Mathematical Society, Providence, 2004).
- [8] Bloch A. M. *Nonholonomic mechanics and control*. – Springer, 2015. – T. 24.
- [9] Borisov A. V., Mamaev I. S. Rolling of a rigid body on plane and sphere. Hierarchy of dynamics. Regular and Chaotic Dynamics. – 2002. – T. 7. – №. 2. – C. 177-200.
- [10] Borisov A. V., Mamaev I. S., Bizyaev I. A., The hierarchy of dynamics of a rigid body rolling without slipping and spinning on a plane and a sphere, *Rus. J. Nonlin. Dyn.*, 2013, Vol. 9, No. 2, pp. 141-202.
- [11] Caughey T. K. A mathematical model of the "rattleback". *International Journal of Non-Linear Mechanics*. – 1980. – T. 15. – №. 4. – C. 293-302.
- [12] Kozlov V. V. On the integration theory of equations of nonholonomic mechanics // *Regul. Chaotic Dyn.* – 2002. – T. 7. – №. 2. – C. 191-176.
- [13] Karapetyan A. V. Hopf bifurcation in the problem of the motion of a heavy rigid body on a rough plane // *Izv. Akad. Nauk SSSR. MTT*. – 1985. – T. 2. – C. 19-24.
- [14] Borisov A.V., Mamaev I.S. Strange attractors in rattleback dynamics. *Physics Uspekhi*, **46**, 2003, 393-403.
- [15] Borisov A.V., Jalnine A.Yu., Kuznetsov S.P., Sataev I.R., Sedova J.V. Dynamical phenomena occurring due to phase volume compression in nonholonomic model of the rattleback. *Regular and Chaotic Dynamics*, **17**, 2012, No 6, 512-532.
- [16] Kuznetsov S.P. On the validity of the nonholonomic model of the rattleback. *Physics-Uspekhi*, **58**, 2015, No 12, 1223-1224.
- [17] Chaplygin S. A. On the theory of motion of nonholonomic systems. The reducing-multiplier theorem // *Regular and Chaotic Dynamics*. – 2008. – T. 13. – №. 4. – C. 369-376.
- [18] Carathéodory C. Der Schlitten // *ZAMM*, 1933, vol. 13, № 2, pp. 71-76.
- [19] Borisov A.V., Mamaev I.S. The dynamics of a Chaplygin sleigh. *Journal of Applied Mathematics and Mechanics*, 2009, Vol. 73, no 2, 156-161.
- [20] Jung P., Marchegiani G., and Marchesoni F. Nonholonomic diffusion of a stochastic sleigh. *Physical Review E*, **93**, 2016, 012606.

- [21] Borisov A.V., Kuznetsov S.P. Regular and Chaotic Motions of a Chaplygin Sleigh under Periodic Pulsed Torque Impacts. *Regular and Chaotic Dynamics*, **21**, 2016, No 7-8, 792–803.
- [22] Ott E., Grebogi C., Yorke J. A. Controlling chaos. *Physical Review Letters*, **64**, 1990, No 11, 1196-1199.
- [23] Pyragas K. Continuous control of chaos by self-controlling feedback. *Physics Letters A*, **170**, 1992, No 6, 421-428.
- [24] Schöll E., Schuster H. G. (ed.). *Handbook of chaos control*. – John Wiley & Sons, 2008.